Electrical and Dielectric Characteristics of Al/Polyindole Schottky Barrier Diodes. II. Frequency Dependence

Seckin Altindal Yeriskin,[1] H. Ibrahim Unal,[2] Bekir Sari[2]

[1]*Department of Chemical Engineering, Faculty of Engineering, Gazi University, Ankara, Turkey*
[2]*Polymers Group, Department of Chemistry, Faculty of Science, Gazi University, Ankara, Turkey*

Received 3 September 2009; accepted 5 August 2010
DOI 10.1002/app.33148
Published online 14 October 2010 in Wiley Online Library (wileyonlinelibrary.com).

ABSTRACT: The dielectric properties and ac electrical conductivity of Al/polyindole (Al/PIN) Schottky barrier diodes (SBDs) were investigated by using admittance spectroscopy (capacitance–voltage [*C*-*V*] and conductance–voltage [*G*/ω-*V*]) method. These *C*-*V* and *G*/ω-*V* characterizations were performed in the frequency range of 1 kHz to 10 MHz by applying a small ac signal of 40 mV amplitude from the external pulse generator, whereas the dc bias voltage was swept from (−10 V) to (+10 V) at room temperature. The values of dielectric constant (ε′), dielectric loss (ε″), dielectric loss tangent (tan δ), real and imaginary part of electrical modulus (M' and M''), ac electrical conductivity (σ_{ac}), and series resistance (R_s) of the Al/PIN SBDs were found to be quite sensitive to frequency and applied bias voltage at relatively low frequencies. Although the values of the ε′, ε″, tan δ, and R_s of the device were observed to decrease with increasing frequencies, the electric modulus and σ_{ac} increased with increasing frequency for the high forward bias voltages. These results revealed that the interfacial polarization can more easily occur at low frequencies and that the majority of interface states (N_{ss}) between Al and PIN, consequently, contribute to deviation of dielectric properties of the Al/PIN SBDs. Furthermore, the voltage-dependent profile of both R_s and N_{ss} were obtained from the *C*-*V* and *G*/ω-*V* characteristics of the Al/PIN SBDs at room temperature.
 J Appl Polym Sci 120: 390–396, 2011

Key words: Al/polyindole Schottky barrier diodes; frequency dependence C-V-f and G/ω-V-f characteristics; dielectric properties; electrical conductivity; series resistance; surface states

INTRODUCTION

Conducting polymers are new materials that have been studied extensively during the last decade.[1] They have been used widely in industrial applications in various fields, such as electronic and electrochromic equipments, photochemical cells, rechargeable batteries, Schottky barrier diodes (SBDs), light-emitting diodes, field effect transistor separation membranes, sensors, and anticorrosive coatings.[2–17] Among these polymers, polyaniline,[18] polypyrrole,[19] polythiophene,[20] and polyindole (PIN)[21] have been studied extensively because of their good conductivity, relatively high environmental stability, nontoxic properties, easily adjustable conducting oxidation states, and simple and economical production routes. PIN is an electroactive polymer, which can be obtained from electrochemical or chemical oxidation of indole monomer (using a suitable oxidant such as $FeCl_3$ or $CuCl_2$).[22]

Vast number of experimental studies in the literature is reported on metal/polymer/semiconductor structures or SBDs in recent years,[2–16] but limited information is available on their temperature,[17] frequency, and applied bias voltage dependence of both electric and dielectric properties in the wide range of frequency and bias voltage. The performance and reliability of these devices depend on various parameters, such as the processing history and impurity level of the material, barrier inhomogeneity and density of the interface states at metal–semiconductor (MS) interface, the serial resistance of the device, device temperature, nature or deposited interfacial insulator layer at MS interface and their homogeneity, and the stability of the polymer used. Therefore, it is important, especially, to include the effect of interface states, series resistance, applied bias voltage, and response of electric and dielectric properties of these devices. To extract as much information as possible, dielectric relaxation spectroscopy data used electric modulus formalism introduced by Macedo et al.[23] Thus, the evaluation of electric modulus as a function of frequency permits to detect the presence of relaxation processes in the studied dielectric materials. Determination of the electric modulus of these materials and their variation with frequency provide a lot of information, which allows

Correspondence to: H. I. Unal (hiunal@gazi.edu.tr).
Contract grant sponsor: Gazi University Research Fund; contract grant number: FEF 05/2006-45.

one to study the relaxation processes for a specific electronic application.[23,24]

The change in the frequency is very important for these structures. In the ideal case, the capacitance of semiconductor structures is usually frequency independent, especially at high-frequency limit ($f \geq$ 1 MHz). However, depending on the frequency of the ac signal, there may be a capacitance because of the interface states in excess to depletion layer capacitance. The reasons for their existence are the interruption of the periodic lattice structure at the surface, surface preparation, formation of the barrier height at meat–organic interface, and impurity concentration of the conducting polymer. In this case, an excess capacitance may occur because of interface states, and it leads to an increase in the real capacitance of the structures. Such changes in the measured capacitance and conductance especially depend on the frequency and applied voltage.[25–29] Also, interface states can easily follow the external ac signal at low frequency and yield an excess capacitance and conductance, which depends on the relaxation time of the interface state and the frequency of ac signal.

In our previous work,[17] we reported the effect of temperature on the main electrical parameters of the Al/PIN-SBDs by using *I-V*, *C-V*, and *G/ω-V* characteristics. In this second part of the study, the frequency and voltage dependence of the both electrical and dielectric parameters such as the series resistance (R_s), interface states (N_{ss}), ac electrical conductivity (σ_{ac}), dielectric constant (ε'), dielectric loss (ε''), loss tangent (tan δ), and the real (M') and imaginary (M'') parts of electric modulus of the Al/PIN-SBDs were investigated. The *C-V* and *G/ω-V* characteristics were investigated in the frequency range of 1 kHz to 10 MHz by applying a small ac signal of 40 mV amplitude from the external pulse generator, whereas the dc bias voltage was swept from (−10 V) to (+10 V) at room temperature. Furthermore, the interface states densities (N_{ss}) of the sample were obtained from the high–low frequency capacitance measurements. Wide-range temperature and voltage-dependent dielectric properties of Al/PIN-SBDs are also under our investigation and will be published soon, as the third part of the study.

EXPERIMENTAL

PIN was chemically synthesized in $CHCl_3$ under a nitrogen atmosphere using $FeCl_3$ as the oxidizing agent at 15°C for 5 hr, taking the ratio of $FeCl_3$ to indole as 3 : 1 with 85% yield and used for fabrication of the SBDs. The full details of the synthesis of PIN were given in our previous article.[17] Al/PIN-SBDs were fabricated by using PIN having a thickness of 1 mm and a diameter of 1 cm. Also, the full details of the fabrication process of this SBDs are reported in our previous study.[17]

The dielectric properties of Al/PIN-SBDs were investigated using *C-V* and *G/ω-V* measurements under both reverse and forward bias in the wide frequency range of 1 kHz to 10 MHz. These measurements were performed by using HP 4192A LF impedance analyzer, which operates in the frequency range of 5 Hz to 13 MHz, and all the measurements were carried out with the help of a microcomputer through an IEEE-488 ac/dc converter card at room temperature. To avoid any contamination on the samples, all measurements were also carried out in a vacuum of $P \leq 10^{-4}$ mmHg.

RESULTS AND DISCUSSION

Frequency dependence of electrical characteristics

The dielectric properties of materials can be expressed in various ways, using different representations. For instance, a comparison of complex dielectric permittivity (ε^*) and electric modulus (M^*) representation allows us to distinguish the local dielectric relation. Therefore, the *C-V* and *G/ω-V* characteristics were performed in the frequency range of 1 kHz to 10 MHz by applying a small ac signal of 40 mV amplitude from the external pulse generator, whereas the dc bias voltage was swept from (−10 V) to (+10 V), and the results obtained are given in Figures 1 and 2, respectively.

As seen in Figure 1(a,b), the values of *C* decrease with increasing frequency and give a broad peak in the range of 1 kHz to 10 MHz. The higher values of *C* and *G/ω* at low frequency region can be attributed to the excess capacitance and conductance resulting from the interface states (N_{ss}) between Al and PIN in Al/PIN-SBD structure. Because, at low-frequency region, the N_{ss} can easily follow the ac signal and, consequently, do contribute appreciably to the diode capacitance.[25–31] However, in the sufficiently high frequency limit ($f \geq 1$ MHz), the N_{ss} almost cannot follow the ac signal; as a result, they do not contribute to the measured capacitance and conductance.

As depicted in Figure 2(a,b), the *G/ω-V* characteristics show similar results in the same frequency range of 1 kHz to 10 MHz. It is clear that under bias voltage, the existence of N_{ss} and their magnitude are responsible for the observed frequency dispersion in *C-V* and *G/ω-V* curves. To clarify, voltage-dependent values of capacitance–frequency (*C-f*) and conductance–frequency (*G/ω-f*) are also given in Figure 3(a,b), at various bias voltages. These very significant data show that a special attention has to be given to the effects of bias voltage on the *C-V* and *G/ω-V* characteristics.

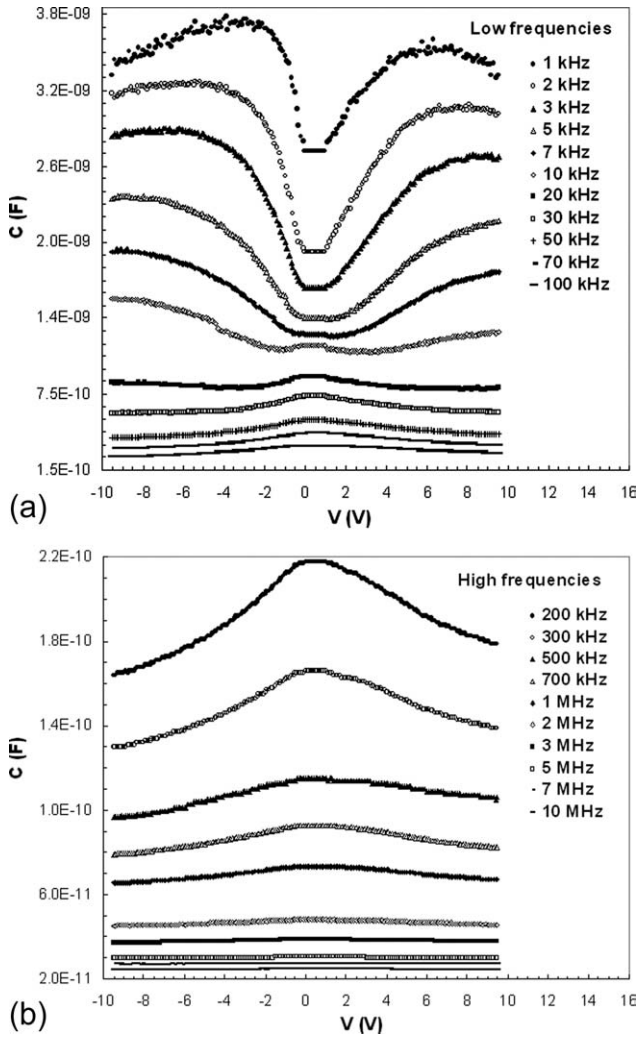

Figure 1 The variation of (a) low- and (b) high-frequency *C-V* characteristics.

As seen in Figure 3(a,b), both the values of C and G/ω decreased with increasing frequency and become almost constant at sufficiently high frequency values ($f \geq 10^6$ Hz). It is clear that the change in C and G/ω is very significant especially at low-frequency region ($f \leq 10^4$ Hz).

Also, the values of series resistance (R_s) are important because they can cause a serious error in the extraction of both electrical and dielectric parameters of the diode from the *C-V* and *G/ω-V* characteristics.[17,25,26,31] Several methods have been suggested in the literature[25,32,33] for the determination of R_s value of MS and metal–insulator–semiconductor type SBDs and metal–oxide–semiconductor capacitors. However, to extract the series resistance of these structures, the method developed by Nicollian and Brews[25] is thought to be generally more accurate than the others. This method provides the determination of R_s in both reverse and forward bias regions and is given as:

$$R_s = \frac{G_m}{G_m^2 + \omega^2 C_m^2} \quad (1)$$

Thus, the series resistance values of the Al/PIN-SBD were calculated from the measured C_m and G_m/ω for each bias voltage in the range of 200 kHz to 10 MHz, and the results obtained are shown in Figure 4. It was observed that the value of R_s decreases with increasing frequency for all the bias voltages, which may be attributed to the particular distribution of N_{ss} and other possible chemical impurities left at Al/PIN interface, during the fabrication. It is clear that the change in R_s is very small at high-frequency region, and it becomes almost independent of applied bias voltage. In this high-frequency range, the interface states cannot follow the ac signal, because the carrier life time (τ) is larger than the measured C_m and G_m/ω period ($T = 1/2\pi f$). Therefore, the real series resistance of the sample can be subtracted from the measured C_m and G_m/ω, especially in the strong accumulation region and at high frequency ($f \geq 1$ MHz).

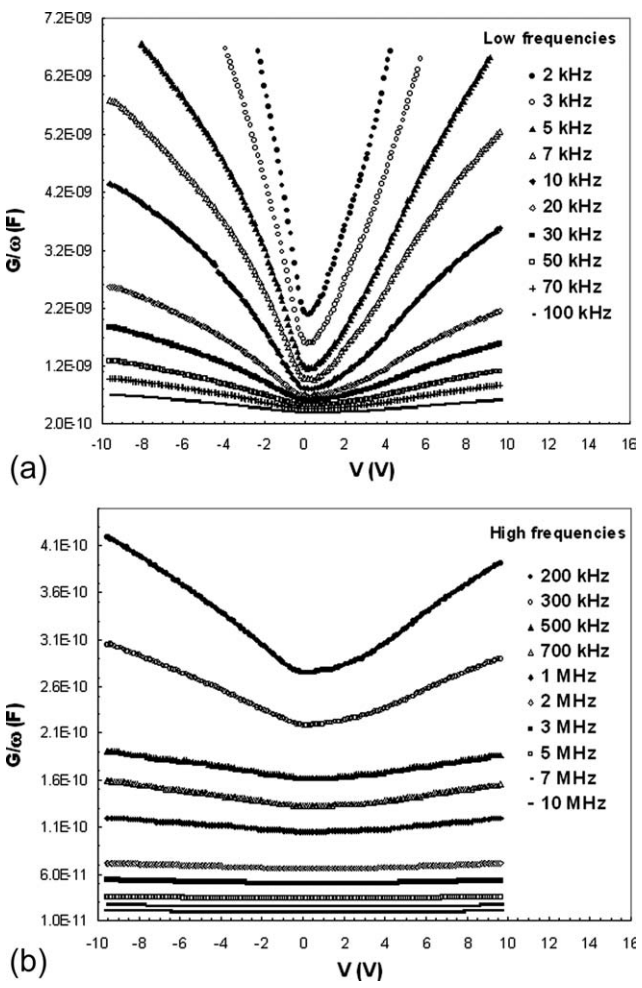

Figure 2 The variation of (a) low- and (b) high-frequency *G/ω-V* characteristics.

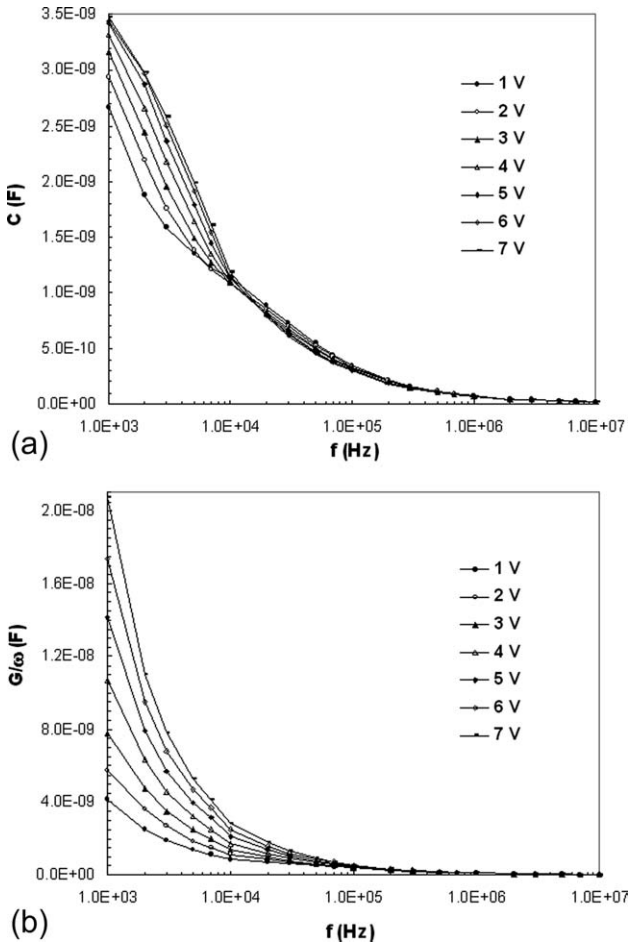

Figure 3 The frequency dependence of (a) *C* and (b) *G*/ω for various bias voltages.

In addition, the distribution of interface states (N_{ss}) profile dependent on the bias voltage was obtained from the measured experimental low–high frequency capacitance (C_{LF}-C_{HF}) method as following[27,28]:

$$N_{ss} = \frac{1}{qA}\left[\left(\frac{1}{C_{LF}} - \frac{1}{C_{PIN}}\right)^{-1} - \left(\frac{1}{C_{HF}} - \frac{1}{C_{ox}}\right)^{-1}\right] \quad (2)$$

where, C_{LF} and C_{HF} are the measured capacitance at low frequency (1 kHz) and at high frequency (1 MHz), respectively, C_{ox} is the interfacial oxide capacitance, A is the area of rectifier contact, and q is the electronic charge. The advantage of this method comes from the fact that it permits determination of many properties of the interfacial insulating or polymer layer very rapidly and accurately. In this method,[25,29] the N_{ss} is extracted from its capacitance contribution to the measured experimental *C*-*V* curve. In the equivalent circuit of MS or metal–insulator–semiconductor type SBDs, the oxide or polymer capacitance is in series with the parallel combination of the interface trap or surface state capacitance (C_{it}) and the space charge capacitance (C_{sc}). In general, in

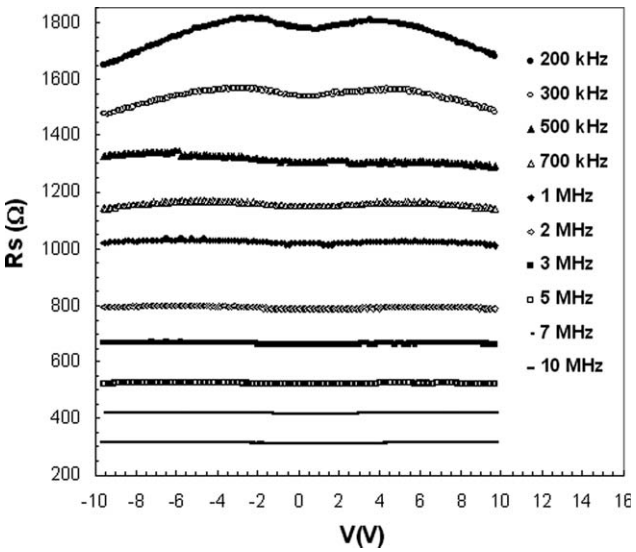

Figure 4 The frequency dependence of R_s.

dark and at high frequency, interface states cannot respond to the ac excitation; thus, they do not contribute to the total capacitance and conductance directly. The density distribution of interface states profile as a function of bias voltage was calculated from eq. (2), and data obtained are shown in Figure 5. The profile of N_{ss} shows U-shape behavior, and the magnitude of N_{ss} is in the order of about 10^{12} eV cm^{-2}, which is not high enough for device applications.

Frequency dependence of the dielectric properties

The values of ε′, ε″, tan δ, σ_{ac}, and the real and imaginary parts of electric modulus (M' and M'') of Al/PIN-SBDs were investigated using the *C*-*V* and *G*/ω-*V* characteristics in the range 1 kHz to 10 MHz,

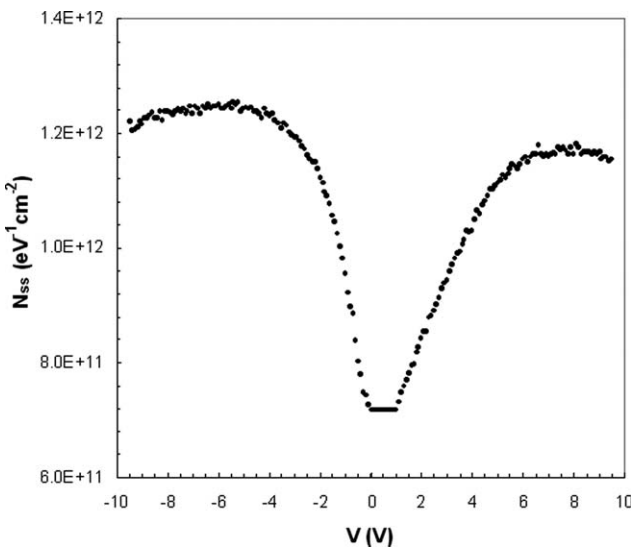

Figure 5 The voltage-dependence profile of N_{ss}.

at room temperature. The complex permittivity (ε*) can be written[34–36] as:

$$\varepsilon* = \varepsilon' - j\varepsilon'' \tag{3}$$

where, ε′ and ε″ are the real and imaginary parts of ε*, respectively, and j is the imaginary root of −1. In the formulation of ε*, in the case of admittance (Y*) measurements, the following relation holds:

$$\varepsilon^* = \frac{Y^*}{j\omega C_0} = \frac{C_m}{C_0} - j\frac{G_m}{\omega C_{oi}} \tag{4}$$

where, C_m and G_m are the measured capacitance and conductance of the sample, and ω is the angular frequency ($\omega = 2\pi f$). Thus, the frequency-dependent ε′ and ε″ for various bias voltages can be calculated using the measured C_m and G_m/ω, respectively, from the relation[34–36]:

$$\varepsilon' = \frac{C}{C_o} = \frac{Cd}{\varepsilon_o A} \tag{5a}$$

$$\varepsilon'' = \frac{G}{\omega C_i} = \frac{Gd_i}{\varepsilon_o \omega A} \tag{5b}$$

where, C_o is the capacitance of an empty capacitor, A is the rectifier contact area of the structure in cm^{-2}, d is the interfacial layer thickness, and ε_o is the permittivity of free space charge ($\varepsilon_0 = 8.85 \times 10^{-14}$ F cm^{-1}). In the strong accumulation region, the maximal capacitance of the structure corresponds to the insulator capacitance ($C_{ac} = C_i = \varepsilon'\varepsilon_0 A/d$). The tan δ can be expressed as[34–39]:

$$\tan\delta = \frac{\varepsilon''}{\varepsilon'} \tag{6}$$

Figure 6(a–c) shows the frequency-dependent values of ε′, ε″, and tan δ curves of the Al/PIN-SBDs at various bias voltages. It was observed that the values of ε′ [Fig. 6(a)] and ε″ [Fig. 6(b)] decreased with increasing frequency, whereas they remained almost constant for all bias voltages at sufficiently high frequency. It is clear that both the values ε′ and ε″ are greater at low frequency because of the possible interface polarization mechanism since N_{ss} cannot follow the ac signal at high frequency. Interface polarization reaches a constant value because beyond a certain frequency of external field the electron hopping cannot follow the alternative field.

In general, at low frequencies, all the four types of polarization processes, i.e., the electronic, ionic, dipolar, and interfacial or surface polarization contribute to the values of ε′ and ε″. With increasing frequency, the contributions of the interfacial, dipolar, or ionic polarization become ineffective by leaving behind only the electronic part. Furthermore, the decrease in ε′ and ε″ with increasing frequency is explained by the fact that as the frequency is raised, the interfacial dipoles have less time to orient themselves in the direction of the alternating field.[40,41] In addition, at high frequencies, the values of ε′ become closer to the values of ε″ because interface states (N_{ss}) at Al/polyindole interface cannot follow the

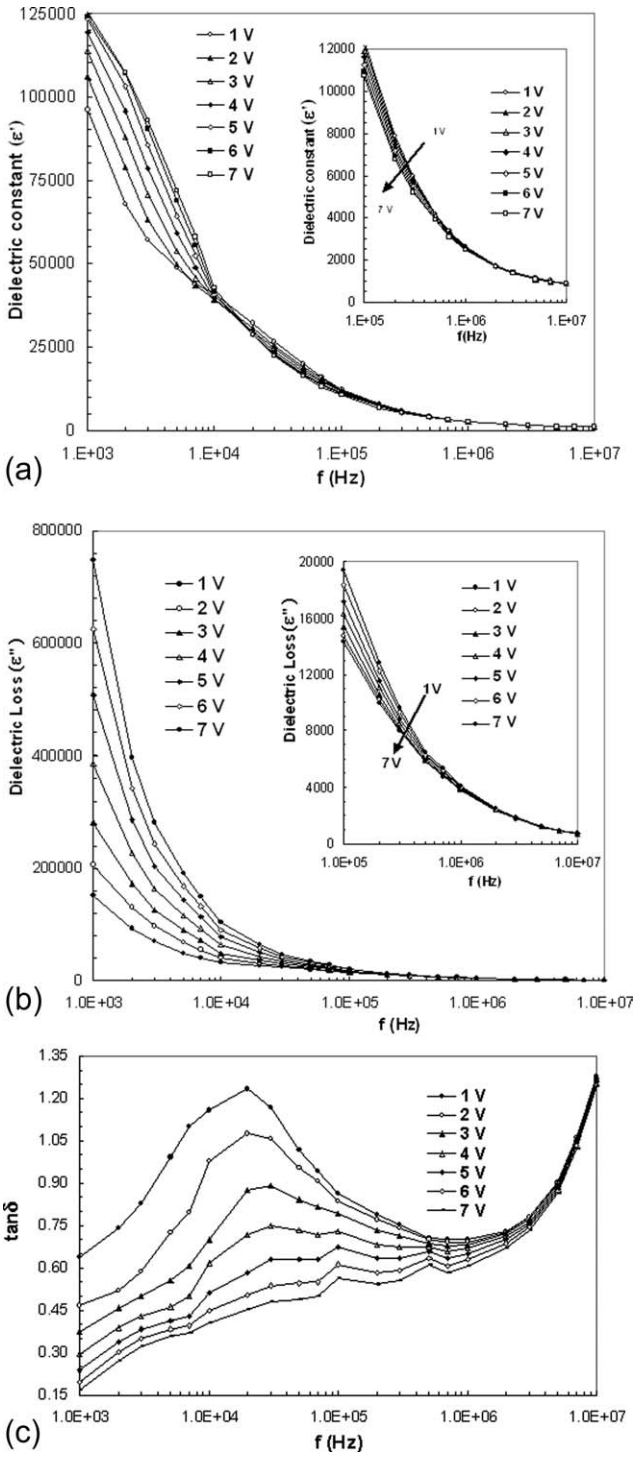

Figure 6 The variation of (a) ε′-f, (b) ε″-f, and (c) tan δ-f for various bias voltages.

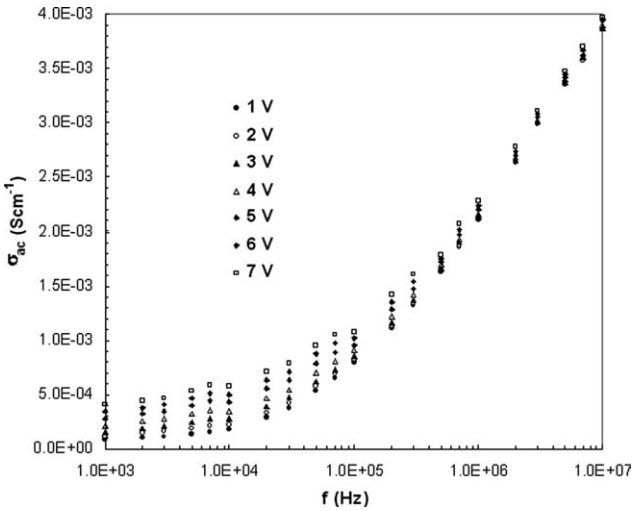

Figure 7 The frequency dependence of σ_{ac} for various bias voltages.

external ac signal. Therefore, the dispersion in ε' and ε'' at low frequencies can be attributed to Maxwell–Wagner-type interfacial polarization, i.e., the fact that inhomogeneities give rise to a frequency dependence of the conductivity because charge carriers accumulate at the boundaries of less-conducting regions, thereby creating interfacial polarization.[40]

These dispersions in ε' and ε'' with frequency can be attributed to Maxwell–Wagner[42] and space–charge polarization.[41] As shown in Figure 6(c), the value of tan δ gives a peak especially for the low bias voltages at about 2 kHz, and, at high frequency, it becomes voltage independent. This behavior of tan δ depends on various parameters such as N_{ss}, R_s, and the thickness of interfacial layer. In the light of experimental results, it can be concluded that the change in frequency and applied bias voltage substantially alters the dielectric parameters of the Al/PIN-SBDs.

The conductivity measured at a particular frequency and temperature is the total conductivity, $\sigma_{total}(\omega)$, of the sample and can be written as[43]:

$$\sigma_{total}(\omega) = \sigma_{ac}(\omega) + \sigma_{dc} \tag{7a}$$

where σ_{dc} and $\sigma(\omega)$ correspond to the respective dc and frequency-dependent ac conductivities. Here, it is assumed that the dc and ac conductivities are due to completely different processes. If the ac and dc conductivities arise because of the same process and σ_{dc} is simply $\sigma_{ac}(\omega)$ in the limit $\omega \rightarrow 0$, then the separation in the above equation is no longer useful. Therefore, the frequency-dependent σ_{ac} of the Al/PIN-SBDs was obtained from eq. (7b),[36–39] for various voltages, and the results obtained are shown in Figure 7.

$$\sigma_{ac} = \omega C \tan\delta\left(\frac{d}{A}\right) = \varepsilon'' \omega \varepsilon_0 \tag{7b}$$

The value of σ_{ac} was observed to increase with increasing frequency. This result is also in accordance with the literature and attributed to the R_s effect.[41] The increase in σ_{ac} with increasing f leads to an increase in the eddy current, which in turn increases in the tan δ.

The complex impedance (Z^*) and complex electric modulus (M^*) formulations were discussed by various authors with regard to the analysis of dielectric materials.[37–41] They preferred to describe the dielectric properties of these devices by using the electric modulus formulation. The complex impedance or the complex permittivity ($\varepsilon^* = 1/M^*$) data are transformed into the M^* formulation using the following relation[37–41]:

$$M^* = \frac{1}{\varepsilon*} = M' + jM'' = \frac{\varepsilon'}{\varepsilon'^2 + \varepsilon''^2} + j\frac{\varepsilon''}{\varepsilon'^2 + \varepsilon''^2} \tag{8}$$

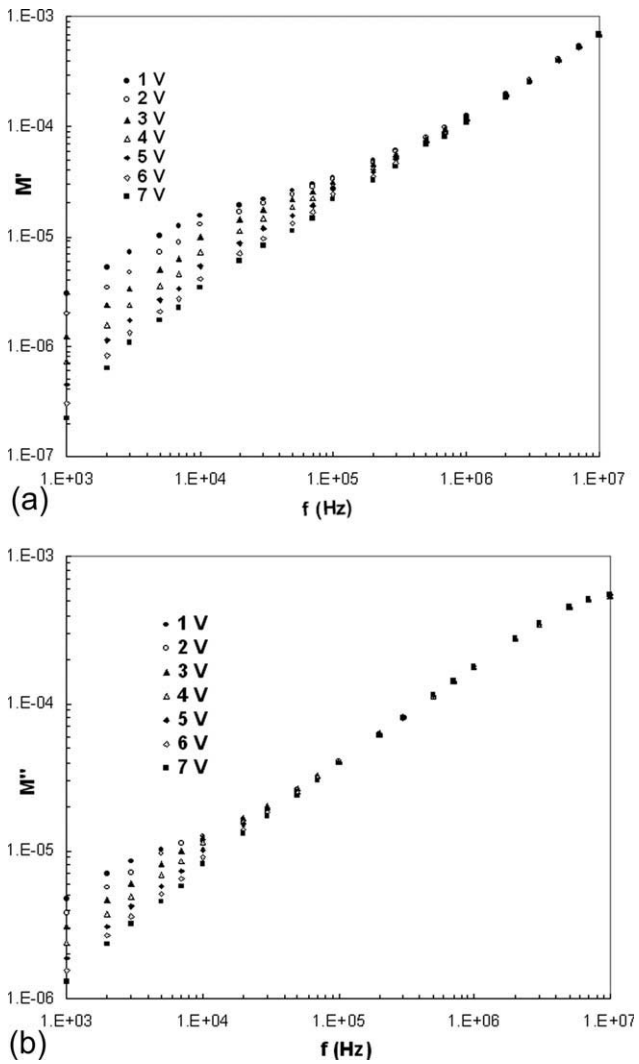

Figure 8 (a) The real part (M′) and (b) the imaginary part (M″) of electric modulus vs. frequency for various bias voltages.

The variation of M' and M'' of the Al/PIN-SBDs as a function of frequency at various bias voltages are given in Figure 8. It is evident that for each bias voltage, both the values of M' and M'' do not reach a maximum value even at higher frequency ($f = 10$ MHz). In other words, M' and M'' reach a maximum constant value corresponding to $M_\infty = 1/\varepsilon_\infty$ because of the relaxation process. On the other hand, the values of both M' and M'' approach almost to zero at low frequency. These results are also consistent with the literature.[36,37,42,44]

CONCLUSIONS

Both the electrical and dielectric parameters such as R_s, N_{ss}, σ_{ac}, ε', ε'', tan δ, M', and M'' of Al/PIN-SBDs were investigated using frequency-dependent *C-V* and *G/ω-V* characteristics in the range of 1 kHz to 10 MHz at room temperature. From analysis of the experimental results it was concluded that the values of ε' and ε'' show a steep decrease with increasing frequency for each bias voltage, whereas the tan δ values show a peak. The interfacial polarization can more easily occur at low frequencies. The values of σ_{ac} were observed to increase with increasing frequency because of the accumulation of charge carriers at the boundaries. Also, the values of M' were found to increase with increasing frequency. These results show that the interfacial polarization can more easily occur at low frequencies and that the majority of N_{ss} at Al/PIN interface, consequently, contribute to the deviation of dielectric properties of the Al/PIN-SBDs. The final remark is that, in the Al/PIN-SBDs, both electrical and dielectric parameters are strongly dependent on both the frequency and applied bias voltage.

References

1. MacDiarmid, A. G. Angew Chem Int Ed 2001, 40, 2581.
2. Abthagir, P. S.; Saraswathi, R. Org Electron 2004, 5, 299.
3. Gupta, R. K.; Singh, R. A. Mater Sci Semicond Process 2004, 7, 83.
4. Abthagir, P. S.; Saraswathi, R. J Mater Sci Mater Electron 2004, 15, 81.
5. Gupta, R. K.; Singh, R. A. Compos Sci Technol 2005, 65, 677.
6. Aydin, M. E.; Yakuphanoglu, F.; Eom, J.; Hwang, D. Physica B 2007, 387, 239.
7. Li-Ming, H.; Ten-Chin W.; Gopalan, A. Thin Solid Films 2005, 473, 300.
8. Akkılıc, K.; Yakuphanoglu, F. Microelectron Eng 2008, 85, 1826.
9. Lee, Y. S.; Park, J. H.; Choi, J. S. Opt Mater 2002, 21, 433.
10. Abthagir, P. S.; Saraswathi, R. J Appl Polym Sci 2001, 81, 2127.
11. Aydogan, S.; Saglam, M.; Türüt, A. Polymer 2005, 46, 563.
12. Paradhan, D. K.; Choudhary, R. N. P.; Samantary, B. K. Mater Chem Phys 2009, 115, 557.
13. Sengwa, R. J.; Choudhary, S.; Sankhla, S. Colloid Surf A: Physicochem Eng Aspects 2009, 336, 79.
14. Tan, C. K.; Blackwood, D. J. Corros Sci 2003, 45, 545.
15. Rajagopalan, R.; Iroh, J. O. Appl Surf Sci 2003, 218, 58.
16. Cho, M. S.; Park, S. Y.; Hwang, J. Y.; Choi, H. J. Mater Sci Eng C 2004, 24, 15.
17. Altindal, S.; Sari, B.; Unal, H. I.; Yavas, N. J Appl Polym Sci 2009, 113, 2955.
18. DeBerry, D. W. J Electrochem Soc 1985, 132, 1022.
19. Beck, F.; Michaelis, R.; Schloten, F.; Zinger, B. Electrochim Acta 1994, 39, 229.
20. Petitjean, J.; Aeiyach, S.; Lacroix, J. C.; Lacaze, P. C. J Electroanal Chem 1999, 478, 92.
21. Sazou, D. Synth Met 2002, 130, 45.
22. Billaud, D.; Maarouf, E. B.; Hannecart, E. Mater Res Bull 1994, 29, 1239.
23. Macedo, P. B.; Moyniham, C. T.; Bose, R. Phys Chem Glasses 1972, 13, 171.
24. McCrum, N. G.; Read, B. E.; Williams, G. Unelastic and Dielectric Effects in Polymeric Solids; Wiley: London, 1967; pp 108–111.
25. Nicollian, E. H.; Brews, J. R. Metal-Oxide-Semiconductor (MOS) Physics and Technology; Wiley: New York, 1982.
26. Sze, S. M. Physics of Semiconductor Devices, 2nd ed.; Wiley: New York, 1981.
27. Deuling, H.; Klausmann, E.; Goetzberger, A. Solid State Electron 1972, 15, 559.
28. Depas, M.; Van Meirhaeghe, R. L.; Lafere W. H.; Cardon, F. Solid State Electron 1994, 37, 433.
29. Castange R.; Vapaille, A. Surf Sci 1971, 28, 157.
30. Varma, S.; Rao, K. V.; Kar, S. J Appl Phys 1984, 56, 2812.
31. Yücedag, I.; Altindal, S.; Tataroglu, A. Microelectron Eng 2006, 84, 180.
32. Sato, K.; Yasamura, Y. J Appl Phys 1985, 58, 3656.
33. Cheung, S. K.; Cheung, N. W. Appl Phys Lett 1986, 49, 85.
34. Symth, C. P. Dielectric Behavior and Structure; McGraw-Hill: New York, 1955.
35. von Hippel, A. R. Dielectric Materials and Applications; John Wiley & Sons: New York, 1954.
36. Fanggao, C.; Saunders, G. A.; Lambson, E. F.; Hampton, R. N.; Carini, G.; Marco, G. D.; Lanza, M. J Appl Polym Sci 1996, 34, 425.
37. Prabakar, K.; Narayandass, S. K.; Mangalaraj, D. Phys Stat Sol 2003, 199, 507.
38. Pissis, P.; Kyritsis, A. Solid State Ionics 1997, 97, 105.
39. Pakma, O.; Serin, N.; Serin, T.; Altindal, S. J Phys D: Appl Phys 2008, 41, 215103.
40. Sattar A. A.; Rahman, S. A. Phys Stat Sol 2003, 200, 415.
41. Afandiyeva, I. M.; Dökme, I.; Altindal, S.; Bülbül, M. M.; Tataroglu, A. Microelectron Eng 2008, 85, 247.
42. Bidault, O.; Goux, P.; Kchikech, M.; Belkaoumi, M.; Maglione, M. Phys Rev B 1994, 49, 7868.
43. Abdel-Wahaby, F. A.; Maksoud, H. M.; Kotkata, M. F. J Phys D: Appl Phys 2006, 39, 190.
44. Kyritsis, A.; Pissis, P.; Grammatikakis, J. J Polym Sci Part B: Polym Phys 1995, 33, 1737.